Slovak University of Technology in Bratislava
Faculty of Mechanical Engineering
19th Conference on Applied Mathematics **APLIMAT 2020**

Proceedings

EXPERIMENTAL 3D SHAPE RECONSTRUCTION FROM HIGH-PRECISION 2D CRUSE SCANS USING SHADOWS AND FOCUSING

POLÁK Mikuláš (SK), PECKO Marcel (SK), BOHDAL Robert (SK), FERKO Andrej (SK)

Abstract. We describe two experiments with the hi-tech CRUSE CS 220ST1100 contactless scanner. The 2D scans guarantee high precision both in geometry and radiometry. The experiments verify the precision of non-standard scanning and two standard object reconstructions. We tested the reconstruction of 3D shape from shadows and from experimental focusing. We discuss educational aspects of given approach within the innovative course on Visual Data of Cultural Heritage.

Keywords: virtual reality, 3D shape reconstruction, shape from shadows

Mathematics Subject Classification: 68U05, 68U07

1 Introduction

In general, in virtual reality and CAD, we minimize errors in the 8-dimensional ($x, y, z, t, r, g, b, \alpha$) parameter space. The α parameter expresses the transparency in an interval [0,1], the (r, g, b) triplet represents colour values, t means time and (x, y, z) denote spatial coordinates in extended Euclidean space. The Cruse CS 220ST1100 contactless scanner solves the error minimization problem by measurement within a 5-dimensional parametric subspace (x, y, r, g, b).

It is possible to scan the given scanline of real artwork under constant illumination accurately up to 1200 pixels per inch in the TIFF format. The scanned original weight may be up to 300 kg, measuring 120×180×30 cm [3, 4]. The current software CSx does not create a 3D model, but allows for precise TIFF scanning with variable illumination, 15-degree sensor rotation and variable depth of field, thus offering dozens of scan versions of a single original. The (r, g, b) colour primaries can be stored in 48-bit colour depth. We study the accuracy of the scan and the speed of the related processes, in order to optimize for given data type [1]. Of course, there exist no absolute exact scanned values, as the CCD “14.400 Pixel Tri Linear RGB Line-Sensor” with Schneider optics has its own limitations. Regardless, the multiple versions of scans motivate the research of possible 3D reconstructions.

We explore two ways how to employ non-standard scanning for estimating the z values. We tested the reconstruction of a shape from shadows and from experimental focusing. We review relevant previous work, in part 2. Part 3 reports on focusing experiments. Part 4 describes the 3D reconstruction from shadows. Finally, we discuss certain educational aspects of given experiments and we identify ideas for future work.

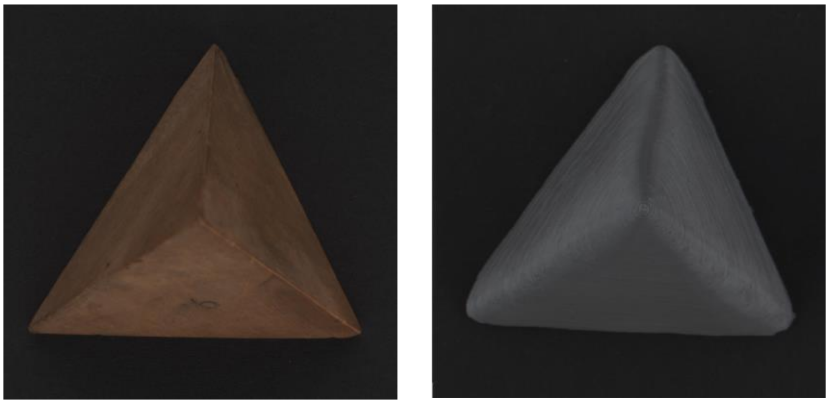

Fig. 1. A real wooden tetraeder and its scanned and 3D printed imitiation [15].

2 Previous Work

Manual focusing of the Cruse scanning using Fourier transform was analyzed by R. Bohdal [1]. The idea of utilizing focusing was proposed by M. Fano in research of confocal microscopy [6]. Using scans for 3D printable prototypes was elaborated by M. Pecko [15]. The shape from shadows idea is known in computer vision research for decades [9]. Utilizing shadows is not supported by standard scanning, but M. Polák has implemented a feasible solution [16].

Within the project *Comeniana – methods and means of digitization and presentation of 3D objects of cultural heritage*, 8 data acquisition modes have been developed and implemented, including Cruse scanning. The most valuable Comenius University heritage items were scanned in a suitable way [17]. For 3D objects no Cruse-based reconstruction was done, but the scans served to reconstruct the lost synagogue hi-precision geometric model in a project of M. Fabian [7]. Worldwide, because of excellent quality, Cruse scans are used to document 2D heritage e.g. in Vatican Secret Archives, NASA, or Pentagon [4]. For scientific processing of images, there are multiple tools recommended, e.g. ImageJ [12]. When dealing with triangular mesh, one can improve and/or measure it using MeshLab [2]. Using photogrammetry, a set of images of given original can be even 3D reconstructed with an on-line service [20].

Visual Data Science is taught at multiple universities. In the year 2019, the Data Science study program was accredited at Comenius University. It will start in academic year 2020-2021. One of the courses is focused to visual data processing for natural and cultural heritage documentation and presentation. "*Processing of big data is becoming a basic building block in all areas thanks to massive development of information technologies*" [21].

Two original Cruse-based workflows were researched and designed by M. Pecko [15] and M. Polák [16], respectively. They focus on geometry and (if there will be the radiometric requirement) the high precision colour from given samples can be used, of course.

3 Focusing experiments for 3D print

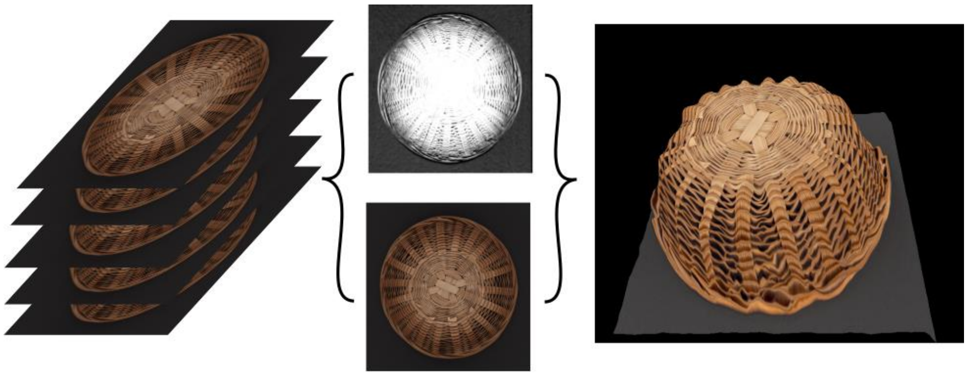

Fig. 2. Focus stacking, depth-of-field and 3D reconstruction of the basket specimen [15].

The well-known description of pushbroom scanner type is given at page 174 in [10]: “a linear sensor array is used... As the sensor moves the sensor plane sweeps out a region of space (hence the name pushbroom), capturing the image... The second dimension of the image is provided by the motion of the sensor. In the linear pushbroom model, the sensor is assumed to move in a straight line at constant velocity with respect to the ground. In addition, one assumes that the orientation of the sensor array with respect to the direction of travel is constant. In the direction of the sensor, the image is effectively a perspective image, whereas in the direction of the sensor motion it is an orthographic projection... Further details on the linear pushbroom camera are given in [8]”. Moreover, technical features of the CRUSE scanner allow to control the height of original and the height of the sensor [3], [15], [19]. We used ***z*** increase by 1 mm. The set of scans is named focus stacking [10]. Fig. 2. illustrates 5 stack items, for each of them one can compute depth of field, and sharpness. The output offers a 3D cloud of points for creation of mesh, which can be converted to STL format [11] for 3D print, see Fig. 1 right. The complete workflow can be summarized in the following steps.

Shape from CRUSE focusing
Input: 3D real world original, ***Output:*** digital twin and 3D printout

1. Selection of the 3D real world original.
2. Scanning of focused image planes into the TIFF format files, using CSx 3.9.
3. Focus stacking, using Helicon Soft. The output is a 3D point cloud in OBJ file format.
4. Triangular mesh processing in Mesh Lab.
5. Converting of meshed object into the STL format (MeshLab).
6. 3D printing of copied original.
7. Intermediate or final results presentation, evaluation, and dissemination.

The workflow is partially illustrated in two figures, Step 1 and Step 6 in Fig 1, Step 3 in Fig 2. Steps 5-6 can be replaced by alternative presentation, e.g. dynamic interactive or animated visualization. For measurement of precision, one can scan the 3D printout again, using the same settings and compute the image differences. However, the rounded edges are noticeable in Fig. 1 left, but the shape of hemisphere in Fig. 5 left is satisfactory.
Steps 2 and 3 depend on focusing, resp. sharpening. Let us have a picture (scan) of $M \times N$ pixels with the intensity values $I(x, y)$, for $x = 0, 1, \ldots, M - 1$ and $y = 0, 1, \ldots, N - 1$. The discrete Fourier transform $F(u, v)$ of the image function $I(x, y)$ is given by

$$F(u,v) = \frac{1}{MN}\sum_{x=0}^{M-1}\sum_{y=0}^{N-1} I(x,y)e^{-i2\pi\left(u\frac{x}{M}+v\frac{y}{N}\right)} \quad (1)$$

and it is plugged into the $S_{ft,1}(x,y)$ sharpness function

$$S_{ft,1}(x,y) = \sum_{u=0}^{M-1}\sum_{v=0}^{N-1}|F(u,v)|, \text{ for } T_{low} < u + v < T_{high}, \quad (2)$$

which allows CSx for manual sharpening [1]. An easier way is by setting the value of Unfocused, see Fig. 3. This parameter is intended for tuning the CRUSE settings in user-friendly way or for special effects.

Fig. 3. Value of Unfocused set to 0.965, 1.001, and 1.800 [15], [16].

In Step 3, the simplest Helicon procedure A uses a non-Fourier computation for given scan. Let *T* be properly chosen threshold and *k* be the size of the difference, usually 1 or 2.

$$S_{df,1}(x,y) = \sum_{x=0}^{M-k-1}\sum_{y=0}^{N-1}|I(x+k,y) - I(x,y)| \text{ or } S_{df,1}(x,y) = \sum_{x=0}^{M-1}\sum_{y=0}^{N-k-1}|I(x,y+k) - I(x,y)|, \quad (3)$$

The thresholding of difference formula (3) for given pixel *I(x,y)* identifies sharp pixels from the others by the Helicon procedure A. The height of given scan we know in advance and this information is encoded in focus stack. Again, we can control the height of reconstructed object by setting it manually. We have to recognize the methods in CSx and Helicon, as they are not published. Helicon offers three methods, named A, B, C. The detailed analysis of sharpening functions offers [1].

We designed a set of experiments to utilize depth-of-field for computing 3D point cloud from geometrically and radiometrically accurate 2D scans. We created our own dataset of the images with different scanner settings CRUSE and various backgrounds. We have compared the 3D models of the scanned objects and compared it its accuracy with the original, even in real world. In total, we created 658 scans representing 35.5 GB of data and we spent tens of hours scanning. These data are intended for future tests and students, see Fig. 3. A sample gallery can be found online at [16]. The survey of measurements offers Tab. 1.

In addition, we even discovered some inaccuracy of the CRUSE device itself. If we run the first scan from point ***A*** to point ***B***, the sliding table remains at point ***B*** and the subsequent scan returns to the reverse in this direction from point ***B*** to point ***A***. In Fig. 4 these positions are next to the black areas (red and green-red line segments). In the reverse scanning, there is a shift of a few pixels, which is not desirable in our experiments. For differences in scans created in two different directions, we found that this offset is approximately 70 pixels, which is not acceptable at all. Therefore, after every single scan, we had to return the table to and scan the object in one direction only. Returning the table to the original position can be achieved by pressing the Move to or Prescan button. This prolonged our experiments, refer to Tab. 1.

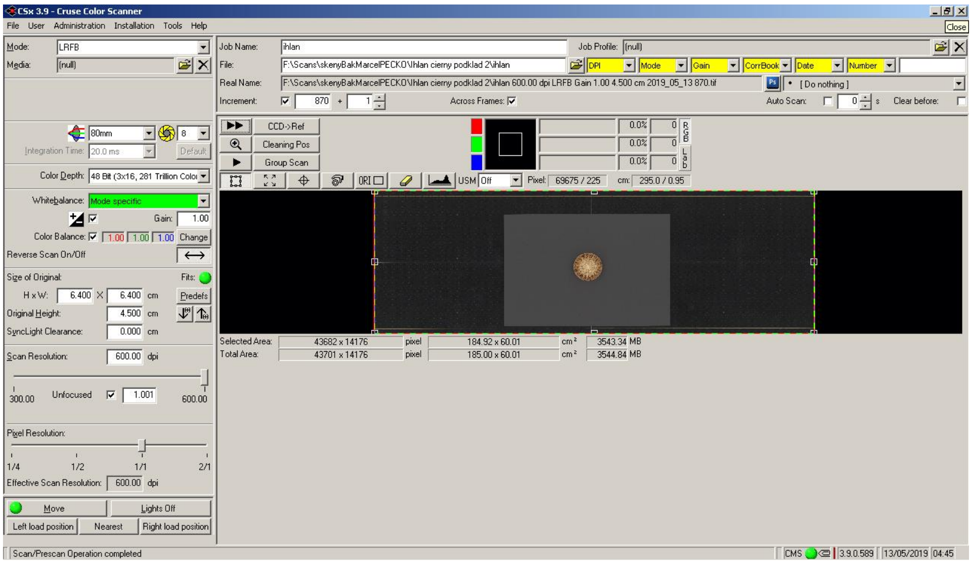

Fig. 4. CSx screenshot during scanning of the basket specimen [15].

SCANNED OBJECTS	BASKET	TETRAEDER	HEMISPHERE
length (mm)	120	47	64
width (mm)	120	54	64
height (mm)	45	45	35
number of scans	46	46	36
size of one scan (MB)	65	13,5	20,5
scan time of one scan (s)	66	29	34

Tab. 1. Scanning times and sizes for LRFB mode [15].

The timing does not include the preparatory times, heating the scanner 30 minutes before each session, experimenting with scanning modes, etc. We concluded, that the LFRB mode giving the illumination from all four sides, maximizes the gain. Printing 3D tetrahedron and hemisphere required another 5 hours. Regardless, we have been able to transfer the confocal microscopy process, which is typically used in the microworld, on a large format CRUSE scanner and we have achieved satisfactory results as a proof of the concept.

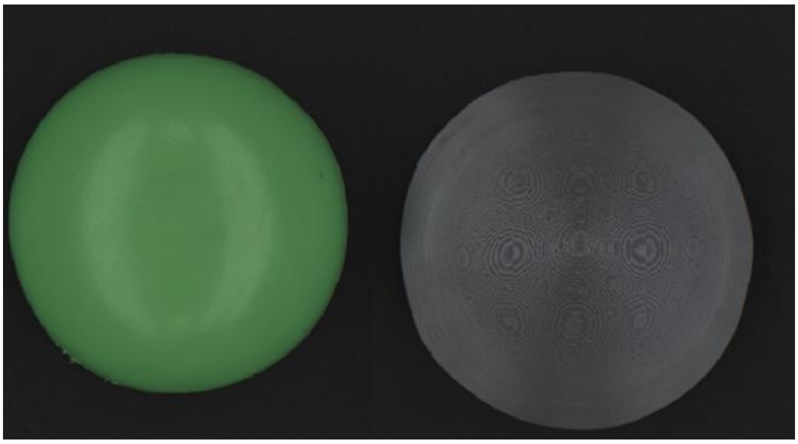

Fig. 5. Hemisphere and its 3D model [15].

4 Shape from Shadows

We analyze algorithm for 3D surface reconstruction using object's shadow to create a program that will process the output images from the CRUSE scanner and build a 3D model of the scanned object [17]. We performed a series of scans of different types of objects under different lighting and we implemented an image processing algorithm. We have to adjust the program to a specific device, and evaluate the effectiveness and accuracy.

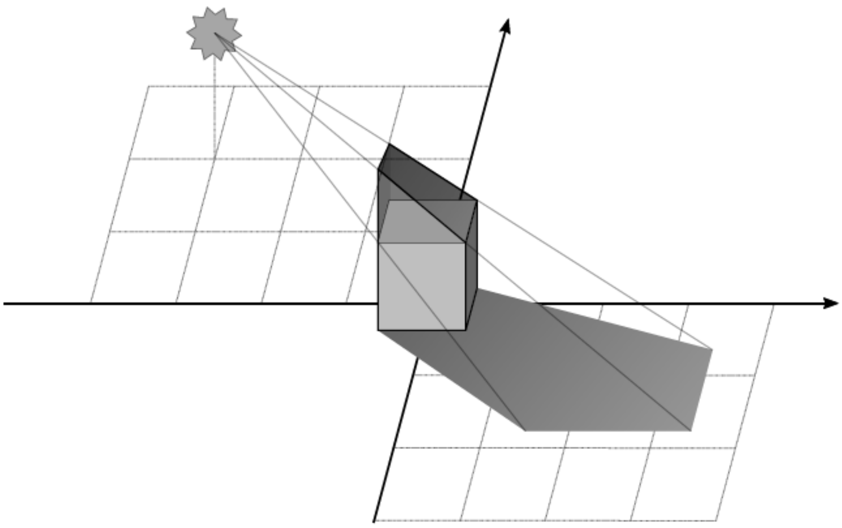

Fig. 6. Cube reconstruction from one shadow [17].

Fig. 6 illustrates the shadow definition for the scene with given point light source.
Definition 1. A portion of a surface is **visible** from a point *X* if every point of the portion of the surface can be connected to *X* without intersecting the surface itself.
Definition 2. A **shadow** is a portion of the surface of the object that is not visible from the light source *L*.
The reconstruction algorithm can be divided into 3 steps [5]:

Shape from CRUSE shadows
Input: 3D real world original scans, ***Output:*** digital twin (point cloud)

1. We search for shadows in the sequence of scans and specify their boundaries. (This step represents image processing itself. As a result, each image will be divided into three items: the scanned object, the shadows and the shadow-free mat. For further computation we will just keep one of these three information for each pixel in a suitable data structure, in other words, it is no longer necessary to work with the image, but sufficient are only these three values.)
2. For each image, we create an object generated by the rays that connect the points shadows with light source. (Naturally, it is sufficient for the object to be generated in where the object is located along the x and y axes. It is shown in Fig. 6 the construction of an object that arises from one shadow of a cube. This property defines a terrain. In each (x, y) position there is a height value greater than or equal to the original scan height.)
3. Create the intersection of all created objects that were created in step 2. The result of this algorithm is a cloud of points determining the object's surface. In other words, each pixel in the image is assigned its height.

The algorithm requires CRUSE scans, but the scanning modes do not support our scenario. In other words, they suppress shadows. We had to modify the scanning process by blocking the CRUSE lamps and employ a separate light source (LED diode with 200 lumens intensity).

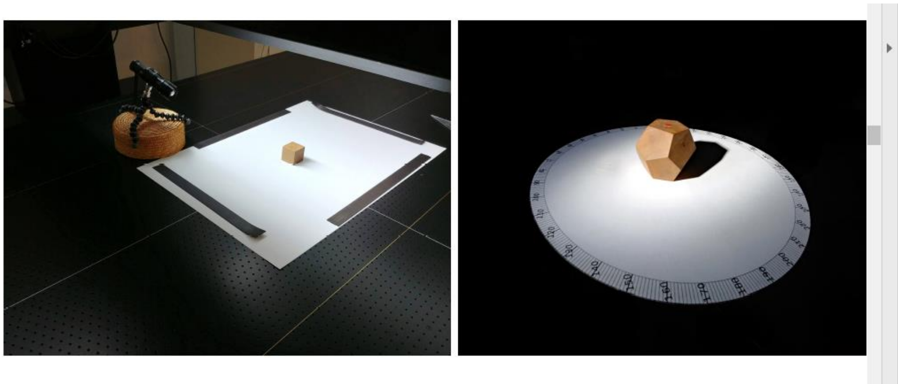

Fig. 7. Our modification of CRUSE scanning set up [17].

Fig. 8. Three test objects with different shadowing properties and added red marker [17].

We selected three objects with different properties, non-convex shape, tetrahedron and a hemisphere. For aligning the coordinate systems, we marked the centre of the scanned scene by a red marker. We have used three coordinate systems in 3D: Cartesian, cylindrical, and spherical. For calibration of scans we inserted a ruler and a goniometer into the scanned scene. The scans we have converted from TIFF into PNG and BMP formats, which were sufficient for our class of precision. The real objects measurements were done with precision 0.5 mm. Our C# program consists of 6 classes (`MainClass.cs`, `Nacitaj.cs`, `Krok1.cs`, `Krok2.cs`, `Krok3.cs`, `Vykresli`). They correspond to the above described approach. The time complexity of the program itself is highest in step 2. Here is for each image time complexity up to O ($nm(n + m)$) where n and m are the sizes of the image in pixels. The memory complexity of the program is equal to the input, i.e. the sum of the sizes of all the images.

We used the Windows 10 Home Edition report to compute and render, Intel Core i7-7700HQ 2.4GHz, 8GB DDR4 memory. We were processing pictures of different sizes up to 4000x4000px. The length of the calculation depended on number of scanned images and the size of those images. For 5 pictures the duration was 1 minute. With 26 scanned images, the calculation lasted up to 5 minutes. This time seems to be long, but because of the time spent during scanning it this is acceptable for the user.

The precision of our models varies with their type. The tetrahedron is damaged by the influence of shadows and the best precision was achieved with the hemisphere model, refer to Fig. 9.

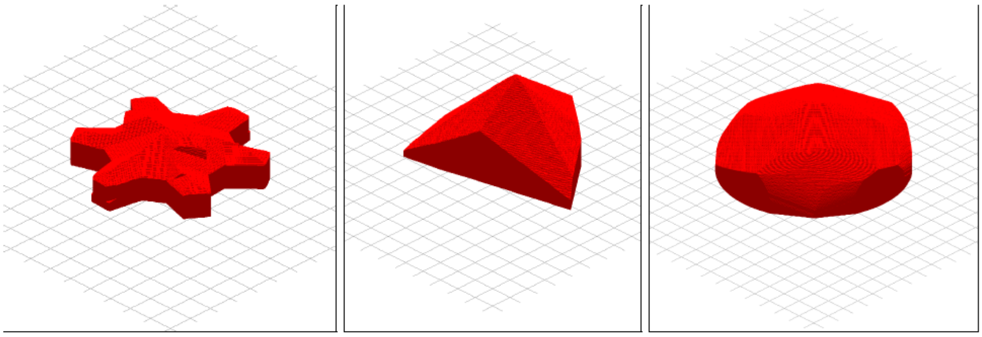

Fig. 9. Three test objects reconstructed and modelled [17].

5 Conclusion and Future Work

The contactless scanning is routinely used for documenting 2D assets of cultural or natural heritage. We have studied the 3D reconstruction hypothesis. The results allow for further study of properties in terms of precision. Both experiments verified the hypothesis, but the amount of needed human work is high and the precision depends on type of the original object. The main contribution we foresee in education. (We test the third alternative, to process CRUSE scans with photogrammetric tools.) Besides the standard 2D documentation and presentation, the content will be enriched by three methods how to profit from scans in the third dimension. The students of Visual Data for Cultural Heritage course will complete one of these projects, using available or new scans and propose their own alterations.

In future research, we intend to scan and reconstruct objects of different shape systematically to study the respective complexity and precision. Of course, we plan to process both datasets using alternative tools to compare the properties of methods. The 48-bit colour precision gives another research direction to combine sufficiently exact geometric shapes with professional colour quality.

Acknowledgement

The CRUSE scanner was supported by Comeniana grant No. ITMS 26240220077 (OPVaV-2011/4.2/07-SORO) and it moved from EDICO SK to FMFI UK. The authors gratefully acknowledge the Scientific Grant Agency KEGA for supporting this work under the Grant No. KEGA 012UK-4/2018 "The Concept of Constructionism and Augmented Reality in the Field of the Natural and Technical Sciences of the Primary Education (CEPENSAR)". Our thanks belong to RNDr. Paula Budzáková for her expertise and kind help with 3D printing.

References

[1] BOHDAL, R. et al. Adaptive Scanning of Diverse Heritage Originals like Synagogue Interior, Empty Rare Papers or Herbarium Items from the 19th Century. *Aplimat 2019.* Bratislava : Slovenská technická univerzita v Bratislave, 2019. pp. 72-82. [USB-key]

[2] CIGNONI, P. et al. MeshLab: an Open-Source Mesh Processing Tool. *Sixth Eurographics Italian Chapter Conference*, pages 129-136, 2008.

[3] Cruse software CSx 3.9. Manual. Wachtberg: CRUSE Spezialmaschinen GmbH., 2018.

[4] CHAMBERS, M. 2018. Pictureelement, *About Our Scans.* [online] http://www.pictureelement.com/aboutcruse.php. (November 15, 2019.)

[5] DICKEY, F. M. and DOERRY, A. W. Recovering shape from shadows in synthetic aperture radar imagery. Proc. *SPIE 6947, Radar Sensor Technology XII*, 694707 (15 April 2008).

[6] FANO, M. *Využitie metód počítačovej grafiky pre rekonštrukciu 3D informácie zo sekvencie 2D rezov*. MSc. thesis. Bratislava: FMFI UK, 2000.

[7] FABIAN, M. 2016. *Virtualizácia bratislavskej synagógy.* Bc. Thesis. Bratislava: FMFI UK, 2019.

[8] GUPTA, R. and HARTLEY, R.I. Linear pushbroom cameras. *IEEE Transactions on Pattern Analysis and Machine Intelligence*.Volume 19, Issue 9, Sep 1997, pages 963 – 975.

[9] HARTLEY, R. and ZISSERMAN, A. *Multiple View Geometry in Computer Vision*. Cambridge University Press, 2003.

[10] Helicon Soft: Kharkiv. [online]. https://www.heliconsoft.com/focus/help/english/HeliconFocus.html. (November 15, 2019.)

[11] HILLER, J. D. and LIPSON, H. Stl 2.0: a proposal for a universal multimaterial additive manufacturing file format. In *Proceedings of the Solid Freeform Fabrication Symposium*, volume 3, pages 266–278, 2009.

[12] ImageJ. https://imagej.net.ImageJ. [online] https://imagej.net. (November 15, 2019.)

[13] LÚČAN, Ľ. *Cruse Scanning Videotutorial.* Bratislava: FMFI UK 2018.

[14] Meshlab. Visual Computing Lab. [online] http://www.meshlab.net/. (November 15, 2019.)

[15] PECKO, M. *Možnosti využitia hlbky ostrosti na analýzu obrazu zo skenera CRUSE a 3D rekonštrukciu.* Bc. Thesis. Bratislava: FMFI UK, 2019.

[16] PECKO, M. Bakalárska práca. http://www.st.fmph.uniba.sk/~pecko7/Bakalarska_praca/Marcel_Pecko.html

[17] POLÁK, M. *Možnosti a charakteristika skenera CRUSE a využitie lokálnych tieňov na analýzu skenovaných objektov.* Bc. Thesis. Bratislava: FMFI UK, 2019.

[18] Project Comeniana Showreel. [online] https://www.youtube.com/watch?v=p7l9iIK88r8. (November 15, 2019.)
[19] RADZIM, P. Poznámky k školeniu CRUSE. Bratislava: FMFI UK, 2018.
[20] VERGAUWEN, M. and VAN GOOL, L. Web-Based 3D Reconstruction Service, *Machine Vision Applications*, 17, pp. 411-426, 2006.
[21] VINAR, T. and HARMAN, R. Data Science. Bachelor's Degree Program (starting in 2020/2021). [online] https://fmph.uniba.sk/en/admissions/bachelors-degree-programs/data-science/ (November 15, 2019.)

Current address

Polák Mikuláš, Bc.
Faculty of Mathematics, Physics and Informatics
Comenius University in Bratislava
Mlynská dolina, 842 48 Bratislava, Slovak Republic
E-mail: polmiki@gmail.com

Pecko Marcel
Faculty of Mathematics, Physics and Informatics
Comenius University in Bratislava
Mlynská dolina, 842 48 Bratislava, Slovak Republic
E-mail: marcelpecko97@gmail.com

Bohdal Robert, RNDr., PhD.
Faculty of Mathematics, Physics and Informatics
Comenius University in Bratislava
Mlynská dolina, 842 48 Bratislava, Slovak republic
E-mail: bohdal@fmph.uniba.sk

Ferko Andrej, doc. RNDr., PhD.
Faculty of Mathematics, Physics and Informatics
Comenius University in Bratislava
Mlynská dolina, 842 48 Bratislava, Slovak Republic
E-mail: ferko@fmph.uniba.sk